CHEMISTRY OF MATERIALS
Cite This: Chem. Mater. 2018, 30, 7521−7526
Article
pubs.acs.org/cm

High-Throughput Identification of Electrides from All Known Inorganic Materials

Lee A. Burton, Francesco Ricci, Wei Chen, Gian-Marco Rignanese, and Geoffroy Hautier*

Institute of Condensed Matter and Nanoscience, Université Catholique de Louvain, 1348 Louvain-la-Neuve, Belgium

Supporting Information

ABSTRACT: In this paper, we present the results of a large-scale, high-throughput computational search for electrides among all known inorganic materials. Analyzing a database of density functional theory results on more than 60 000 compounds, we identify 65 new electride candidates and recover 4 already known. We report on all these candidates and discuss the structural and chemical factors leading to electride formation. Among these candidates, our work identifies the first partially filled 3d transition-metal-containing electrides Ba_3CrN_3 and Sr_3CrN_3, an unexpected finding that contravenes conventional chemistry.

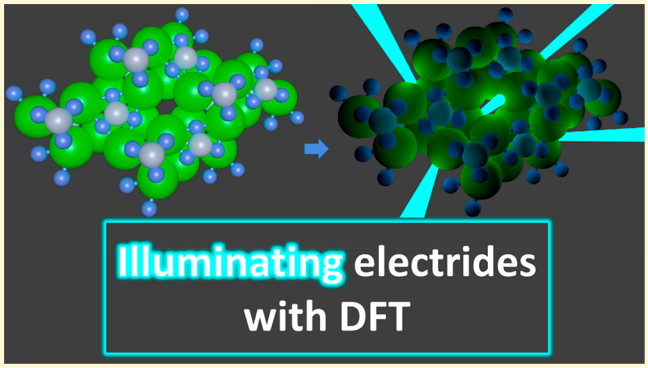

INTRODUCTION

Electrides are rare ionic compounds in which an electron does not occupy an atomic orbital but rather acts as an anion. Such an electron is expected to behave differently from those occupying the valence state of standard materials, making electrides desirable as electron emitters,[1] nonlinear optical switches,[2] superconductors,[3] battery anodes,[4] and catalysts for applications ranging from compound synthesis to CO_2 splitting.[5,6]

Chemically independent electrons were first reported from salts of metal−ammonia solutions.[7] Solid-state organic electrides were reported in 1990 but were unstable at room temperature even in inert atmosphere.[8] In 2012, a breakthrough came with the first inorganic electride stable at room temperature and in air: $Ca_{12}Al_{14}O_{32}$ in the mayenite structure.[9] Now, various stable electrides are known. They are often classified according to the localization of the anionic electron in the lattice: 0-dimensional (0D)[10] when it resides in a cavity, 1-dimensional (1D)[11] when it is enclosed in a channel, and 2-dimensional (2D)[12] when it is confined to a layer. These compounds are now being tested in multiple industrial applications from NH_3 catalysis,[13] to light emitting diode (LED) devices.[14] As such, electride chemistry has become an active field of solid-state chemistry and materials science with large efforts directed toward their discovery, synthesis, and characterization.

Several simple rules have been used to identify possible electride candidates. First, the structure must contain free space where the anionic electron can reside,[8] be this a cavity, a channel, or a layer. Second, a compound must have an excess electron to contribute to the lattice, as determined by the sum of oxidation states of the components.[15] Finally, the compound must contain a strongly donating cation to offset the naturally large energy of a unbound electron.[15] For example, the 2D electride Ca_2N has two Ca^{2+} cations and one N^{3-} anion (according to commonly held concepts of oxidation state). The electropositive Ca cations wish to donate four electrons, but the anion can only accept three, leading to an excess electron occupying free space in the crystal structure, thereby satisfying all three criteria. The need for these three factors to combine adequately makes electrides a rare occurrence among solid compounds with only a handful electrides known so far.

Quantum-mechanical calculations have been essential in the quest for new electrides. They are commonly used in conjunction with experimental characterization (e.g., catalytic activity or transport measurements) to demonstrate the electride nature of a material. By observing the localization of electrons resulting from computations in the density functional theory (DFT) framework, one can determine if the electrons occupy space away from a nuclei, the definition of an electride.[16,17] *Ab initio* techniques have been used extensively in the past to predict electride-like behavior in high-pressure elements.[18−21] However, no large-scale, broad computationally driven search for electrides has yet been performed among known, stable, inorganic compounds at ambient pressure.

Here, we search for potential electrides among a large database containing DFT electronic structure data on materials originating mainly from those experimentally reported in the Inorganic Crystal Structure Database (ICSD).[22] From this database of more than 60 000 compounds, we identify 65 new potential electrides and recover 4 already known, without

Received: June 15, 2018
Revised: October 9, 2018
Published: October 10, 2018

DOI: 10.1021/acs.chemmater.8b02526
Chem. Mater. 2018, 30, 7521−7526

relying on any of the design principles associated with their usual discovery. We discuss the 3 most popular groups of candidates, which incidentally form 0D, 1D, and 2D electrides. Furthermore, we highlight what we believe to be the only known instances of electrides containing a redox active element: Ba_3CrN_3 and Sr_3CrN_3 (significant as one would expect a redox active transition metal to accept the anionic electron). Finally, we re-evaluate the previously proposed guiding principles for electride formation in light of our large-scale screening.

METHODS

Our computational screening began with the Materials Project,[22] a database of 69 640 materials computed using the Vienna *ab initio* Simulation Package (VASP) using the GGA-PBE implementation of DFT.[23,24] Of these, we exclude materials of just one component, i.e., elements, and those with a calculated energy above the convex hull of more than 24 meV per atom, which has been shown to be an accurate measure of stability in compounds.[25] We focused on materials with the Fermi level (E_F) crossing several bands of the compounds that have calculated band structures, i.e., metals. The first screening step was using the projections on atomic orbitals for the eigenstates around E_F in a range of 0.01 eV. If these projections summed to less than 50% of the total electrons present, we expect a high chance for the electrons to occupy nonatomic sites and, thus, be an electride. In a second step, we performed a Bader charge analysis to identify electron distributions with a relative charge of at least 0.1 located 2.2 Å or more away from the nearest atom,[26−28] within 0.2 eV of the E_F for a 2000 k points per $Å^{-3}$ resolution calculation,[29] similar to alternate work in the field.[30,31] The parameters were chosen to return as few candidates as possible while still recovering the four known electrides Ca_2N,[32] Y_2C,[33] Y_5Si_3,[16] and LaH_2,[34] identifying 69 nonelemental candidates in total. We note that only "as-is" electrides will be found through our approach and that we do not expect to find mayenite, for instance, which requires a chemical treatment (oxygen deintercalation) to produce its electride form.[35]

The quasiparticle self-consistent GW (QSGW) calculations were performed using ABINIT.[36] The dielectric function and quasiparticle self-energies are evaluated on a 4 × 4 × 6 k-point mesh and with 1000 bands (see Supporting Information for the convergence study). The energy cutoff for the dielectric function is 160 eV. The semicore sp electrons are included among valence for the Ba, Sr, and Cr atoms.[37] In addition to all the valence states, we include 80 unoccupied states for which the wave functions and eigenvalues are iterated to self-consistency. The virtue of QSGW (compared to one-shot G_0W_0) is that when self-consistency is reached, all remnants of the DFT starting point are eliminated.

RESULTS

Our screening begins with the Materials Project database, which includes DFT electronic structure data for a large set of known materials. By analyzing the charge density around the Fermi level for all stable metallic materials within this database, we can detect the compounds presenting the off-nuclei electron localization characteristic of an electride (see Methods). Our search identifies 69 compounds with 4 previously reported electrides among them (Ca_2N,[32] Y_2C,[33] Y_5Si_3,[16] and LaH_2[34]). We stress that, contrary to previous materials discovery work in electrides,[17,38] we do not look for hypothetical yet-to-be-synthesized phases. Instead, we search among previously known inorganic materials for those presenting electride behavior. The full list of the 69 candidates, their structures, band diagrams, and free electron densities can be found in the Supporting Information.

The most common structure among the top electrides is found for equiatomic binary species. These are PrGa, CaAu, NdGa, CaSi, SrSn, BaGe, SrGe, CaGe, BaSi, SrSi, and BaSn, which are orthorhombic with the space group *Cmcm* (No. 63). The structures consist of bonded atomic bilayers sandwiched between 2D free electron layers (see Figure 1) and are referred

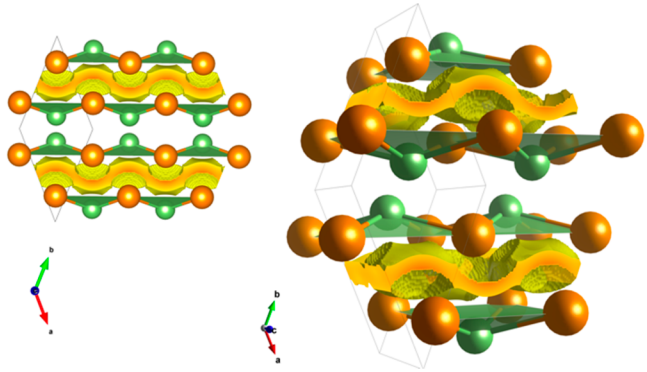

Figure 1. Electron density around the Fermi level for the CrB class candidates clearly indicative of a 2D electride material (NdGa in this case).

to as CrB-type structures in the original reports. Of these 11, 8 are II−IV compounds, complying with the principle of including an electropositive element (group II) in the compound. However, the rule of an excess electron from the oxidation states does not apply. To the knowledge of the authors, these compounds have never been considered electrides but show 2D behavior similar to that of the well-studied Ca_2N.

Of the 69 systems, 9 adopt the so-called Mn_5Si_3 structure type, including the known electride Y_5Si_3, which is reported to be chemically stable even in the presence of moisture.[16] These are Ba_5As_3, Ca_5Sb_3, Nd_5Ge_3, Sr_5As_3, Y_5Si_3, Sr_5Sb_3, Sr_5Bi_3, Ba_5Bi_3, and Ba_5Sb_3, all of which are hexagonal with the space group $P6_3/mcm$ (No. 193). Of the 9 compounds, 7 are II−V compounds. In the unit cells, 3 of 5 cations sit at the center of face-sharing octahedra, while the remaining 2 coordinate toward a 1D channel populated by the anionic electron, see Figure 2.

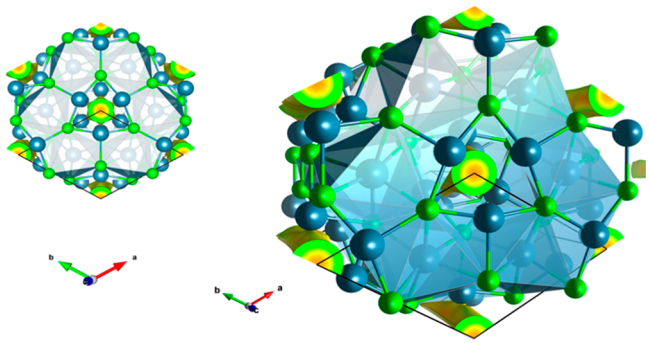

Figure 2. Structure and electron density channel (perpendicular to the page) for the Mn_5Si_3 compounds (Ba_5As_3 in this case).

Eight of the systems are tetragonal Cr_5B_3 compounds with the space group $I4/mcm$ (No. 140). These are La_5Si_3, Ba_5Sn_3, Sr_5Sn_3, Sr_5Ge_3, Ca_5Ge_3, Ca_5Au_3, Sr_5Si_3, and Ca_5Si_3. Most of these systems (6/8) are II−IV compounds, as are those of the CrB-type, the exceptions being, in both cases, either Au or f-block elements. Their structure consists of complete and

DOI: 10.1021/acs.chemmater.8b02526
Chem. Mater. 2018, 30, 7521−7526

partial octahedra, i.e., 5-coordinated cations in distorted square-based pyramid polyhedra, where the base of the pyramid orients toward a cavity containing localized electron distribution, see Figure 3. The anionic electron completes an octahedral coordination environment for the cation, itself being 4-coordinated.

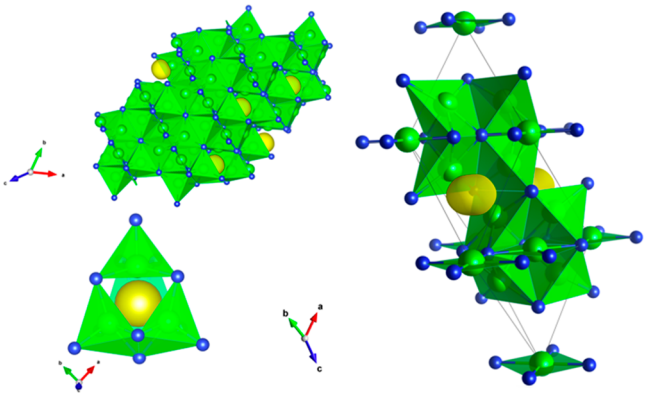

Figure 3. (Top left) the supercell structure of Sr_5Si_3 (Sr as green, Si as blue), (right) the unit cell, and (bottom left) the immediate bonding environment of the 0D free electron density, yellow.

The previous discussion has focused on the 3 most common groups by structure type in our results. Subsequently, we highlight two compounds identified by our method that would be the first electrides to contain redox active elements: Ba_3CrN_3 and Sr_3CrN_3. These nitrides exhibit structures composed of trigonal planar Cr and pseudotetrahedral coordinated cations (Ba/Sr) in a hexagonal system with the space group $P6_3/m$ (No. 176), see Figure 4. In this case, each Ba/Sr is exposed to a 1D anionic electron, similar to the Mn_5Si_3 compounds.

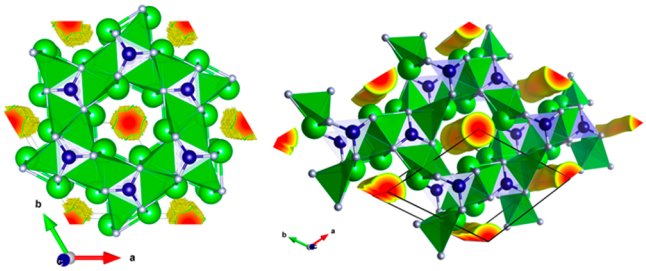

Figure 4. One-dimensional electride behavior in Ba_3CrN_3 and Sr_3CrN_3: Ba/Sr (green), Cr (blue), N (white).

DFT can sometimes fail in representing the electronic structure for systems containing transition metal elements with localized d electrons. Hence, we also compute the electronic structure of the two Cr compounds using many-body perturbation theory,[39,40] within the quasiparticle self-consistent GW (QSGW) approximation. This theory dramatically improves agreement with experiments[41,42] and is a superior level of treatment to, for example, hybrid levels of theory, as no property-dependent parametrization is required.[43,44] We find that while the QSGW slightly shifts the valence band and the conduction band with respect to the PBE band structure, the band gap remains closed at the A point for both compounds (see Supporting Information). In addition, the same 1D free electron channels are also predicted by the QSGW charge density, confirming the electride behavior of Ba_3CrN_3 and Sr_3CrN_3 with one of the highest levels of theory available.

DISCUSSION

So far, the Cr compounds we identified have not been considered as electrides although bond valence calculations performed in the original report indicated an overall excess electron for the compound based on obtained charges of 4.17 and 4.11 for Cr in Sr_3CrN_3 and Ba_3CrN_3, respectively (assuming Sr/Ba^{2+} and N^{3-}).[45] While the authors note that "the values deviate significantly from the expected oxidation states", they ascribe such deviations to bond covalency. They also note the absence of Jahn−Teller distortion for the Cr coordination that one might expect for low-spin d^3 Cr^{III} but attribute this to a difference in size for the alkaline-earth cations. Our results indicate an alternative explanation, whereby Cr^{IV} is formed with an anionic electron in the channel. This finding is counterintuitive as it could be expected that the energy induced by changing the redox active Cr from +3 to +4 would always be more favorable than delocalizing an electron in the crystal structure, as has been reported explicitly for high-pressure electrides.[46]

This leads to a broader discussion about how the electride nature of these 65 candidates was overlooked in the literature. We note that most of the papers reporting on these compounds only discuss synthesis conditions and crystallography. No electron distribution characterization or *ab initio* computing is usually provided, and therefore, the electride character of the compound could not be detected. It is interesting though to observe that many of the electrides are reported as Zintl phases (at least 13 of the 69), which are defined as compounds of element groups I−II bonded with elements from groups III−VII.[47] Such species can defy rules of common oxidation states by the coordination of multiple anions together in order to satisfy their own electron counting rules.[48] However, it can be seen in the structures of our candidates that they do *not* exhibit anion aggregation and possess a structural dependence on electron density to reduce repulsion between cations. An alternative explanation often reported relates to the presence of unidentified H^- in the structure. This has explicitly been claimed in the literature for the Mn_5Si_3 class of compounds[49] and is seen for example with A_5X_3H, in which H can stabilize ternary phases that do not exist for the corresponding A_5X_3 binaries.[50] It is impossible to discount the presence of H in the original experimental structures, but we offer evidence to support our assignment as electrides. The first is that, according to DFT, all compounds in this study are stable or almost stable versus decomposition to competing phases (see Supporting Information). The second is that we successfully recover known electrides. Finally, it has been demonstrated that hydrogen can be removed selectively by chemical treatment from electrides as has been deemed essential to the catalytic activity of Ca_2N.[51]

We also take advantage of our large data set to revisit the established design principles for electrides, i.e., the presence of a strongly electropositive elements, nonmatching oxidation states, and cavities in the structure. There is a consistent inclusion of electropositive elements in our candidates, but it is broader in scope than has been considered in the past. While the most common group is the alkaline-earth metals, the rare-earth elements and alkaline metals are also represented; it is interesting to note that only 1 candidate contains Li. Perhaps this principle can even be extended to the exclusion of

DOI: 10.1021/acs.chemmater.8b02526
Chem. Mater. 2018, 30, 7521−7526

electronegative elements as there are zero chalcogenide- or halogen-containing compounds in our candidates. Instead we see nitrides, silicides, or germanides as common anions.

The most popular group of candidates in this study do not follow the rule of excess electron in the sum of oxidation states. In fact, only 17 of the 69 results have common oxidation states summing to +1 (Ba_5As_3, La_5Si_3, Ca_5Sb_3, Ba_3CrN_3, Sr_3CrN_3, Sr_5As_3, LaH_2, Y_5Si_3, Ca_2N, Sr_5Bi_3, Ba_5Bi_3, La_3Tl, Ca_2Bi, Pr_3Tl, Sr_5Si_3, Ca_5Si_3, Ba_5Sb_3,). We note however that in many cases oxidation state assignment can be extremely ambiguous.[52] Moreover, there are many materials with apparently non-matching oxidation states that are not electrides, such as La_3Te_4.[53] Alternate studies in the field have relied explicitly on this design principle,[17,54] which our results show can limit the scope of discovery significantly. While it is possible to argue many different charge state summations for each case, we believe that this principle should be set aside in the pursuit of new electrides.

The necessity for cavities in the crystal system is somewhat corroborated by our results. For example, the CrB-type compounds do show an interlayer spacing. However, simple consideration of large voids is insufficient. Looking at the bonded plane perpendicular to the 1D electron density in Ca_5Sb_3, as an example, it is possible to see that the anionic electron resides in one of the smaller pores of the structure (see Figure 5) as the electron distribution allows the cations to

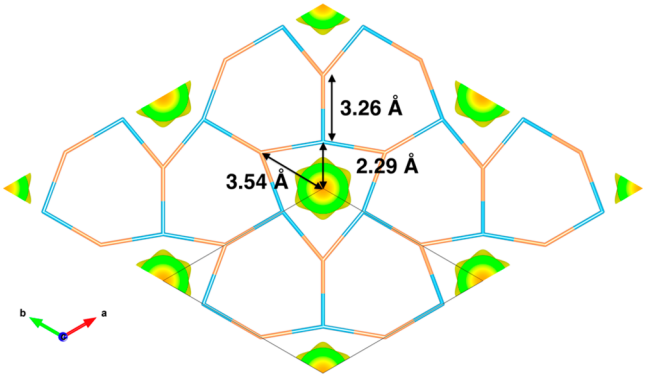

Figure 5. Relevant interspecies distances for the bonded plane of Ca_5Sb_3 showing the smaller pore size around the free electron. The electron density around the Fermi level is also shown.

draw closer together. Indeed, the cation−electron distance is even smaller than the cation−anion distance. Similarly, in the structure for Sr_5Si_3 (Figure 3), the bonds between the cation and the anion are 3.30 and 3.43 Å whereas the distances between the cation and electron are 2.68 and 2.77 Å. Also, this extends to the 2D electrides, where the interlayer spacing is less than those observed in standard 2D materials such as MoS_2. This concept has been arrived upon for high-pressure electrides previously, whereby it was observed that pore space for anionic electron occupation "only becomes important when the size of the enclosed space becomes comparable to the size of typical atoms".[55] These distances indicate that the anionic electrons are volumetrically rather small, which is surprising as there is no positive nucleus contracting the electron distribution about a point in space. Such a behavior is problematic in terms of independent identification of electrides from structure alone, as 3D structure vacancies of the order of the material's bond length or smaller are ubiquitous in materials science.

Finally, while in this work the candidates are grouped on the basis of structure, structure does not necessarily define electride behavior. In our study K_3Rb and Ca_3Tl have identical structures and formula types but present entirely different electron densities around the Fermi level. K_3Rb shows a diffuse distribution whereas Ca_3Tl exhibits very clear 1D electride behavior, as shown in Figure 6. This can also be seen in the different anion−electron coordination environments found for identical structures (see Supporting Information).

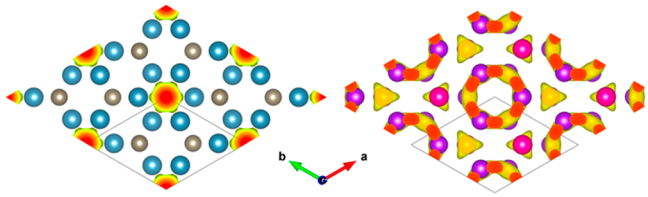

Figure 6. Top-down electron density around the Fermi level within the same range of the Fermi energy for compounds with identical structure and formula type Ca_3Tl (left) and K_3Rb (right).

The main text of this paper discusses in detail less than half of the total number of candidates. However, we believe that we have adequately illustrated that the true extent of electride materials has until now been incredibly limited and refer the reader to the Supporting Information for electronic structure results and valence electron density presented on an individual basis. Further details can also be found here, for example, three candidates (Nd_3In, Sr_5Bi_3, and $Sr_{11}Mg_2Si_{10}$) exhibit band splitting for spin-up and spin-down states, which is evidence of bulk magnetism.

One apparent oversight of our work is the electrides Sr_2N and Ba_2N, which we do not recover. Electronic structure calculations performed by others have predicted the existence of electrons between the layers of atoms in Sr_2N,[56] and Ba_2N,[31] a prediction that is supported by X-ray and ultraviolet photoemission spectroscopy,[57] and neutron diffraction experiments.[58] However, in the Materials Project database these compounds do not yet have computed band structures and, as such, were excluded from our work. We could manually add these compounds to the study, but we instead opt to use these as examples to highlight one of the intrinsic flaws of any high-throughput study, the finite nature of any data set. That said, we would like to stress that the absence of these systems in no way invalidates the materials that we do identify as electrides; it merely points to the existence of even more electrides in nature than we find here.

In summary, while the rules of electride identification can be instructive, they ought not limit the consideration of new and existing materials. We propose that many candidates have long been known, but difficulties in observing electron density around the Fermi level in experiments mean electrides have been overlooked in the past. As such, high-throughput studies such as this are critical for uncovering powerful new functionalities of solid-state systems for a wide variety of applications. By revisiting systems not considered in this way before, we find new electrides that do not have oxidation states indicating an excess electron, that contain redox active transition metals and have narrow cavities in the crystal structure. Combined with such a large number of potential

DOI: 10.1021/acs.chemmater.8b02526
Chem. Mater. 2018, 30, 7521−7526

candidates, we show that these industry-relevant materials are much wider in scope and accessibility than ever illustrated before. It is expected that the compounds discussed in this paper will be of importance for a wide variety of applications and the fundamental understanding of materials.

■ ASSOCIATED CONTENT

Supporting Information

The Supporting Information is available free of charge on the ACS Publications website at DOI: 10.1021/acs.chemmater.8b02526.

Structures and band diagrams for the full list of 69 candidate electrides, information from the original experimental reports, and convergence data for the self-consistent GW calculations (PDF)

■ AUTHOR INFORMATION

Corresponding Author

*E-mail: geoffroy.hautier@uclouvain.be.

ORCID

Lee A. Burton: 0000-0002-0647-5483
Francesco Ricci: 0000-0002-2677-7227
Wei Chen: 0000-0002-7496-0341
Gian-Marco Rignanese: 0000-0002-1422-1205
Geoffroy Hautier: 0000-0003-1754-2220

Notes

The authors declare no competing financial interest.

■ ACKNOWLEDGMENTS

Computer resources were provided by the Université Catholique de Louvain (CISM/UCL) and the Consortium des Equipements de Calcul Intensif en Fédération Wallonie Bruxelles (CECI) funded by the F.R.S.-FNRS. G.-M.R. is grateful to the F.R.S.-FNRS for financial support. Financial support from the F.R.S.-FNRS is acknowledged through the projects HTBaSE. The Materials Project is funded by the U.S. Department of Energy, Office of Science, Office of Basic Energy Sciences, Materials Sciences and Engineering Division, under Contract DE-AC02-05-CH11231: Materials Project program KC23MP.

■ REFERENCES

(1) Huang, R. H.; Dye, J. L. Low Temperature (−80°C) Thermionic Electron Emission from Alkalides and Electrides. *Chem. Phys. Lett.* **1990**, *166*, 133−136.

(2) He, H.-M.; Li, Y.; Yang, H.; Yu, D.; Li, S.-Y.; Wu, D.; Hou, J.-H.; Zhong, R.-L.; Zhou, Z.-J.; Gu, F.-L.; et al. Efficient External Electric Field Manipulated Nonlinear Optical Switches of All-Metal Electride Molecules with Infrared Transparency: Nonbonding Electron Transfer Forms an Excess Electron Lone Pair. *J. Phys. Chem. C* **2017**, *121*, 958−968.

(3) Hosono, H.; Kim, S.-W.; Matsuishi, S.; Tanaka, S.; Miyake, A.; Kagayama, T.; Shimizu, K. Superconductivity in Room-Temperature Stable Electride and High-Pressure Phases of Alkali Metals. *Philos. Trans. R. Soc., A* **2015**, *373*, 2037.

(4) Hu, J.; Xu, B.; Yang, S. A.; Guan, S.; Ouyang, C.; Yao, Y. 2D Electrides as Promising Anode Materials for Na-Ion Batteries from First-Principles Study. *ACS Appl. Mater. Interfaces* **2015**, *7*, 24016−24022.

(5) Ye, T.-N.; Li, J.; Kitano, M.; Hosono, H. Unique Nanocages of $12CaO{\cdot}7Al_2O_3$ Boost Heterolytic Hydrogen Activation and Selective Hydrogenation of Heteroarenes over Ruthenium Catalyst. *Green Chem.* **2017**, *19*, 749−756.

(6) Toda, Y.; Hirayama, H.; Kuganathan, N.; Torrisi, A.; Sushko, P. V.; Hosono, H. Activation and Splitting of Carbon Dioxide on the Surface of an Inorganic Electride Material. *Nat. Commun.* **2013**, *4*, 2378.

(7) Jortner, J.; Kestner, N. R. *Electrons in Fluids: The Nature of Metal-Ammonia Solutions*; Springer: Berlin, 1973.

(8) Dye, J. L. Electrides: Ionic Salts with Electrons as the Anions. *Science* **1990**, *247*, 663.

(9) Kitano, M.; Inoue, Y.; Yamazaki, Y.; Hayashi, F.; Kanbara, S.; Matsuishi, S.; Yokoyama, T.; Kim, S.-W.; Hara, M.; Hosono, H. Ammonia Synthesis Using a Stable Electride as an Electron Donor and Reversible Hydrogen Store. *Nat. Chem.* **2012**, *4*, 934−940.

(10) Matsuishi, S.; Toda, Y.; Miyakawa, M.; Hayashi, K.; Kamiya, T.; Hirano, M.; Tanaka, I.; Hosono, H. High-Density Electron Anions in a Nanoporous Single Crystal: $[Ca_{24}Al_{28}O_{64}]4+(4e-)$. *Science* **2003**, *301*, 626.

(11) Zhang, Y.; Xiao, Z.; Kamiya, T.; Hosono, H. Electron Confinement in Channel Spaces for One-Dimensional Electride. *J. Phys. Chem. Lett.* **2015**, *6*, 4966−4971.

(12) Lee, K.; Kim, S. W.; Toda, Y.; Matsuishi, S.; Hosono, H. Dicalcium Nitride as a Two-Dimensional Electride with an Anionic Electron Layer. *Nature* **2013**, *494*, 336−340.

(13) Kanbara, S.; Kitano, M.; Inoue, Y.; Yokoyama, T.; Hara, M.; Hosono, H. Mechanism Switching of Ammonia Synthesis Over Ru-Loaded Electride Catalyst at Metal−Insulator Transition. *J. Am. Chem. Soc.* **2015**, *137*, 14517−14524.

(14) Hosono, H.; Kim, J.; Toda, Y.; Kamiya, T.; Watanabe, S. Transparent Amorphous Oxide Semiconductors for Organic Electronics: Application to Inverted OLEDs. *Proc. Natl. Acad. Sci. U. S. A.* **2017**, *114*, 233−238.

(15) Zhang, Y.; Wang, H.; Wang, Y.; Zhang, L.; Ma, Y. Computer-Assisted Inverse Design of Inorganic Electrides. *Phys. Rev. X* **2017**, *7*, 1.

(16) Lu, Y.; Li, J.; Tada, T.; Toda, Y.; Ueda, S.; Yokoyama, T.; Kitano, M.; Hosono, H. Water Durable Electride Y_5Si_3: Electronic Structure and Catalytic Activity for Ammonia Synthesis. *J. Am. Chem. Soc.* **2016**, *138*, 3970−3973.

(17) Tada, T.; Takemoto, S.; Matsuishi, S.; Hosono, H. High-Throughput Ab Initio Screening for Two-Dimensional Electride Materials. *Inorg. Chem.* **2014**, *53*, 10347−10358.

(18) Pickard, C. J.; Needs, R. J. Dense Low-Coordination Phases of Lithium. *Phys. Rev. Lett.* **2009**, *102*, 146401.

(19) Neaton, J. B.; Ashcroft, N. W. Pairing in Dense Lithium. *Nature* **1999**, *400*, 141−144.

(20) Takemura, K.; Christensen, N. E.; Novikov, D. L.; Syassen, K.; Schwarz, U.; Hanfland, M. Phase Stability of Highly Compressed Cesium. *Phys. Rev. B: Condens. Matter Mater. Phys.* **2000**, *61*, 14399−14404.

(21) Ma, Y.; Eremets, M.; Oganov, A. R.; Xie, Y.; Trojan, I.; Medvedev, S.; Lyakhov, A. O.; Valle, M.; Prakapenka, V. Transparent Dense Sodium. *Nature* **2009**, *458*, 182−185.

(22) Jain, A.; Ong, S. P.; Hautier, G.; Chen, W.; Richards, W. D.; Dacek, S.; Cholia, S.; Gunter, D.; Skinner, D.; Ceder, G.; et al. Commentary: The Materials Project: A Materials Genome Approach to Accelerating Materials Innovation. *APL Mater.* **2013**, *1*, 011002.

(23) Kresse, G.; Furthmüller, J. Efficient Iterative Schemes for *Ab Initio* Total-Energy Calculations Using a Plane-Wave Basis Set. *Phys. Rev. B: Condens. Matter Mater. Phys.* **1996**, *54*, 11169−11186.

(24) Kresse, G.; Joubert, D. From Ultrasoft Pseudopotentials to the Projector Augmented-Wave Method. *Phys. Rev. B: Condens. Matter Mater. Phys.* **1999**, *59*, 1758−1775.

(25) Hautier, G.; Ong, S. P.; Jain, A.; Moore, C. J.; Ceder, G. Accuracy of Density Functional Theory in Predicting Formation Energies of Ternary Oxides from Binary Oxides and Its Implication on Phase Stability. *Phys. Rev. B: Condens. Matter Mater. Phys.* **2012**, *85*, 155208.

(26) Henkelman, G.; Arnaldsson, A.; Jónsson, H. A Fast and Robust Algorithm for Bader Decomposition of Charge Density. *Comput. Mater. Sci.* **2006**, *36*, 354−360.

DOI: 10.1021/acs.chemmater.8b02526
Chem. Mater. 2018, 30, 7521−7526

(27) Tang, W.; Sanville, E.; Henkelman, G. A Grid-Based Bader Analysis Algorithm without Lattice Bias. *J. Phys.: Condens. Matter* **2009**, *21*, 084204−084207.
(28) Sanville, E.; Kenny, S. D.; Smith, R.; Henkelman, G. Improved Grid-Based Algorithm for Bader Charge Allocation. *J. Comput. Chem.* **2007**, *28*, 899−908.
(29) Sun, W.; Dacek, S. T.; Ong, S. P.; Hautier, G.; Jain, A.; Richards, W. D.; Gamst, A. C.; Persson, K. A.; Ceder, G. The Thermodynamic Scale of Inorganic Crystalline Metastability. *Sci. Adv.* **2016**, *2*, e1600225−e1600225.
(30) Kitano, M.; Kanbara, S.; Inoue, Y.; Kuganathan, N.; Sushko, P. V.; Yokoyama, T.; Hara, M.; Hosono, H. Electride Support Boosts Nitrogen Dissociation over Ruthenium Catalyst and Shifts the Bottleneck in Ammonia Synthesis. *Nat. Commun.* **2015**, *6*, 6731.
(31) Walsh, A.; Scanlon, D. O. Electron Excess in Alkaline Earth Sub-Nitrides: 2D Electron Gas or 3D Electride? *J. Mater. Chem. C* **2013**, *1*, 3525.
(32) Gregory, D. H.; Bowman, A.; Baker, C. F.; Weston, D. P. Dicalcium Nitride, Ca_2N—a 2D ″Excess Electron″ Compound; Synthetic Routes and Crystal Chemistry. *J. Mater. Chem.* **2000**, *10*, 1635−1641.
(33) Zhang, X.; Xiao, Z.; Lei, H.; Toda, Y.; Matsuishi, S.; Kamiya, T.; Ueda, S.; Hosono, H. Two-Dimensional Transition-Metal Electride Y_2C. *Chem. Mater.* **2014**, *26*, 6638.
(34) Mizoguchi, H.; Okunaka, M.; Kitano, M.; Matsuishi, S.; Yokoyama, T.; Hosono, H. Hydride-Based Electride Material, LnH_2 (Ln = La, Ce, or Y). *Inorg. Chem.* **2016**, *55*, 8833−8838.
(35) Lee, D.-K.; Kogel, L.; Ebbinghaus, S. G.; Valov, I.; Wiemhoefer, H.-D.; Lerch, M.; Janek, J. Defect Chemistry of the Cage Compound, $Ca_{12}Al_{14}O_{33}$−δ—Understanding the Route from a Solid Electrolyte to a Semiconductor and Electride. *Phys. Chem. Chem. Phys.* **2009**, *11*, 3105.
(36) Gonze, X.; Amadon, B.; Anglade, P.-M.; Beuken, J.-M.; Bottin, F.; Boulanger, P.; Bruneval, F.; Caliste, D.; Caracas, R.; Côté, M.; et al. ABINIT: First-Principles Approach to Material and Nanosystem Properties. *Comput. Phys. Commun.* **2009**, *180*, 2582−2615.
(37) van Setten, M. J.; Giantomassi, M.; Bousquet, E.; Verstraete, M. J.; Hamann, D. R.; Gonze, X.; Rignanese, G. M. The PSEUDODOJO: Training and Grading a 85 Element Optimized Norm-Conserving Pseudopotential Table. *Comput. Phys. Commun.* **2018**, *226*, 39−54.
(38) Zhang, Y.; Wang, H.; Wang, Y.; Zhang, L.; Ma, Y. Computer-Assisted Inverse Design of Inorganic Electrides. *Phys. Rev. X* **2017**, *7*, 011017.
(39) Hedin, L.; Lundqvist, S. Effects of Electron-Electron and Electron-Phonon Interactions on the One-Electron States of Solids. *Solid State Phys.* **1970**, *23*, 1−181.
(40) Onida, G.; Reining, L.; Rubio, A. Electronic Excitations: Density-Functional versus Many-Body Green's-Function Approaches. *Rev. Mod. Phys.* **2002**, *74*, 601−659.
(41) van Schilfgaarde, M.; Kotani, T.; Faleev, S. Quasiparticle Self-Consistent GW Theory. *Phys. Rev. Lett.* **2006**, *96*, 226402.
(42) Kümmel, S.; Kronik, L. Orbital-Dependent Density Functionals: Theory and Applications. *Rev. Mod. Phys.* **2008**, *80*, 3−60.
(43) Ernzerhof, M.; Perdew, J. P.; Burke, K. Coupling-Constant Dependence of Atomization Energies. *Int. J. Quantum Chem.* **1997**, *64*, 285−295.
(44) Ernzerhof, M.; Scuseria, G. E. Assessment of the Perdew−Burke−Ernzerhof Exchange-Correlation Functional. *J. Chem. Phys.* **1999**, *110*, 5029.
(45) Barker, M. G.; Begley, M. J.; Edwards, P. P.; Gregory, D. H.; Smith, S. E. Synthesis and Crystal Structures of the New Ternary Nitrides Sr_3CrN_3 and Ba_3CrN_3. *J. Chem. Soc., Dalton Trans.* **1996**, *47*, 1.
(46) Miao, M.-S.; Hoffmann, R. High Pressure Electrides: A Predictive Chemical and Physical Theory. *Acc. Chem. Res.* **2014**, *47*, 1311−1317.
(47) Fässler, T.; Evers, J. *Zintl Phases: Principles and Recent Developments*; Springer, 2011.
(48) Sevov, S. C. Zintl Phases. In *Intermetallic Compounds—Principles and Practice*; John Wiley & Sons, Ltd.: Chichester, UK; pp 113−132.
(49) Leon-Escamilla, E. A.; Corbett, J. D. Hydrogen in Polar Intermetallics. Binary Pnictides of Divalent Metals with Mn_5Si_3-Type Structures and Their Isotypic Ternary Hydride Solutions. *Chem. Mater.* **2006**, *18*, 4782−4792.
(50) Leon-Escamilla, E. A.; Corbett, J. D. Hydrogen Stabilization.:-Nine Isotypic Orthorhombic A_5Pn_3H Phases (among A = Ca, Sr, Ba, Sm, Eu, Yb; Pn = Sb, Bi) Formerly Described as Binary β-Yb_5Sb_3-Type Compounds. *J. Alloys Compd.* **1998**, *265*, 104−114.
(51) Kitano, M.; Inoue, Y.; Ishikawa, H.; Yamagata, K.; Nakao, T.; Tada, T.; Matsuishi, S.; Yokoyama, T.; Hara, M.; Hosono, H. Essential Role of Hydride Ion in Ruthenium-Based Ammonia Synthesis Catalysts. *Chem. Sci.* **2016**, *7*, 4036−4043.
(52) Catlow, C.; Stoneham, A. Ionicity in Solids. *J. Phys. C: Solid State Phys.* **1983**, *16*, 4321−4338.
(53) May, A. F.; Fleurial, J.-P.; Snyder, G. J. Thermoelectric Performance of Lanthanum Telluride Produced via Mechanical Alloying. *Phys. Rev. B: Condens. Matter Mater. Phys.* **2008**, *78*, 125205.
(54) Walsh, A.; Scanlon, D. O. Electron Excess in Alkaline Earth Sub-Nitrides: 2D Electron Gas or 3D Electride? *J. Mater. Chem. C* **2013**, *1*, 3525.
(55) Miao, M.; Hoffmann, R. High-Pressure Electrides: The Chemical Nature of Interstitial Quasiatoms. *J. Am. Chem. Soc.* **2015**, *137*, 3631−3637.
(56) Fang, C. M.; de Wijs, G. A.; de Groot, R. A.; Hintzen, H. T.; de With, G. Bulk and Surface Electronic Structure of the Layered Sub-Nitrides Ca_2N and Sr_2N. *Chem. Mater.* **2000**, *12*, 1847−1852.
(57) Steinbrenner, U.; Adler, P.; Hölle, W.; Simon, A. Electronic Structure and Chemical Bonding in Alkaline Earth Metal Subnitrides: Photoemission Studies and Band Structure Calculations. *J. Phys. Chem. Solids* **1998**, *59*, 1527−1536.
(58) Brese, N. E.; O'Keeffe, M. Synthesis, Crystal Structure, and Physical Properties of Sr_2N. *J. Solid State Chem.* **1990**, *87*, 134−140.

DOI: 10.1021/acs.chemmater.8b02526
Chem. Mater. 2018, 30, 7521−7526